Dynamic Fracture and Matrix Heterogeneity and Remaining Oil Models of Ultra-Low Permeability Reservoir

Li Liu[(✉)], Youjing Wang, and Jiahong Li

Research Institute of Petroleum Exploration and Development, Beijing, China
{Liuli85,wangyoujing,lijia-hong}@petrochina.com.cn

Abstract. The ultra-low permeability reservoir is rich in resource, but with the development of oilfield water flooding, contradictions are becoming more and more obvious, resulting from heterogeneity of thick sandstones and dynamic fractures. In order to solve the above problems, this paper takes HuaQing B153 block as an example, based on the study of sedimentary facies and reservoir architecture, the origin type, geometry, size of a single sandbody and the spatial superimposed styles, with its effects on the reservoir connectivity, are determined, and matrix heterogeneity is figured out. In combination with the characteristics and distribution of dynamic fractures and nature fractures, the relationship between dynamic fractures with natural fractures, single sandbody configurations, and reservoir heterogeneity parameters is clearly pointed out. In the following, four remaining oil distribution patterns are established controlled by the dynamic fracture and reservoir matrix heterogeneity, including (1) model integrating dynamic fracture—natural fracture(siltstone)—composite single sandbody—siltstone; (2) model integrating dynamic fracture—natural fracture (top calcite)—siltstone—composite single sandbody; (3) model integrating dynamic fracture—natural fracture (base calcite)—siltstone—composite single sandbody; and (4) model integrating dynamic fracture—natural fracture (siltstone)—siltstone—single sandbody. These models will instruct well pattern adjustment and the remaining oil potential prediction.

Keywords: Ultra-low permeability reservoir · Sandy debris flow · Dynamic fracture · Matrix heterogeneity · Remaining oil model

1   Introduction

The low-permeability reservoirs in the Ordos Basin are rich in resources and have great potential for development. In this basin, they are expected to have proven reserves of 3.54 billion tons and proven reserves of 820 million tons. Chang 6_3 reservoir in Huaqing B153 block is a typical ultra-low permeability reservoir, and it has been developed effectively. However, after a period of production, some development conflicts have become increasingly prominent, mainly in the following two aspects: (1) water flooding occurs in multiple directions, and the water content is greater than 95%. In some wells, water injection is not effective, which leads to a reduction of plane sweep efficiency; (2) affected by dynamic fractures and the heterogeneity of the matrix reservoir, the injecting water runs along the fractures or high-permeability zones, resulting in water flooding and non-uniform development in thick sandy debris flow reservoirs.

In order to solve these problems, this paper focuses on the geometry, scale and spatial configuration of single sandbody of gravity flow, and its influence on reservoir heterogeneity, discuss the heterogeneity of dynamic fractures and matrix reservoirs, establish bins of dynamic fractures and matrix reservoirs and the remaining oil distribution model under different control factors. This paper will provide basis for well pattern adjustment.

2   Geology and Development

The B153 block is located in the Yishan slope of eastern part of Ordos Basin [1]. The tectonic structure is a simple monocline, gently dipping to west, with a dip angel less than 1° (Fig. 1). The Chang 6_3 reservoir in this area is a typical ultra-low permeability reservoir with normal ground temperature (3.2 °C/100 m) and low formation pressure (initial pressure coefficient = 0.79). Chang 6_3 reservoir is sandy debris flow or turbidity sediment and is divided into six layers, including Chang 6_3^{11}, Chang 6_3^{12}, Chang 6_3^{21}, Chang 6_3^{22}, Chang 6_3^{31} and Chang 6_3^{32}, all of which are divided into two sub-layers. The rock type is mainly feldspar sandstone or lithic feldspathic sandstone, fine grained, with a grain size range of 0.07–0.16 mm; the average porosity is 9.47%, and the average permeability is 0.34×10^{-3} μm^2, with strong reservoir heterogeneity. In addition, natural fractures along EW or NE develop in upper Chang 6_3 reservoir, enhancing the heterogeneity of the reservoir. The B153 block takes inverted nine spot injection pattern to develop and has undergone four development stages, including the exploratory well production phase, the comprehensive production construction phase, the water flooding phase and the production plateau stage.
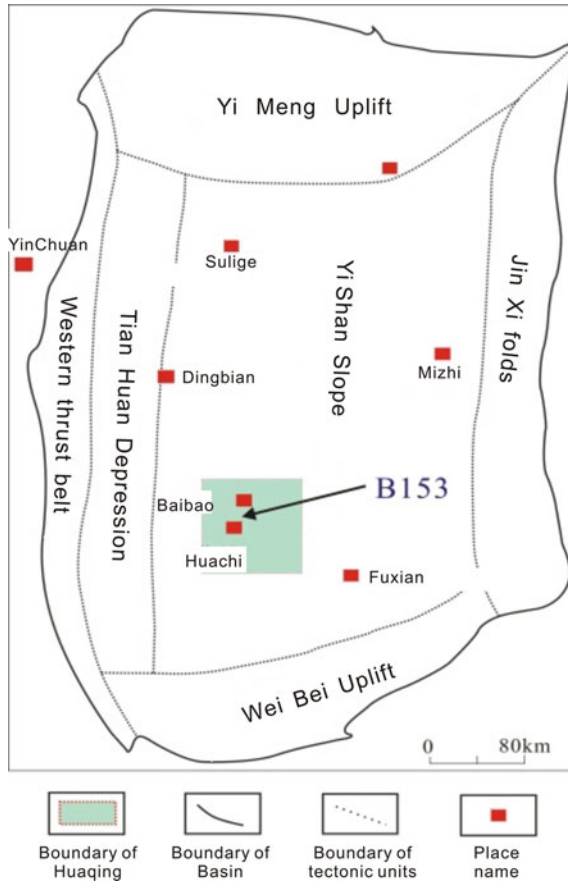
Fig. 1. Tectonic units and location of B153 block

3 Dynamic Fracture Characteristics and Heterogeneity Characterization

3.1 Definition

Dynamic fracture is a new development geological property of ultra-low permeability reservoirs [2]. It was closed at the original state, but with the increase of injection pressure and formation pressure, the formation at the bottoms of injection cracked and formed fractures [3–5], which can extend and communicate with each other. Both the geometric parameters and permeability of these fractures behave dynamic changes. The formation of dynamic fractures leads to a step shaped increase of water content between major oil wells, but the sweep effect of lateral oil wells is not obvious. Therefore, the dynamic fracture is the most import heterogeneity parameter in the late development stage of ultra-low permeability reservoir. The prediction of the remaining oil distribution is of great significance.

3.2   Identification of Dynamic Fractures

The dynamic fractures can be identified comprehensively by using well loggings, interwell interference well test, tracer analysis, water injection profiles, and production performances of production and injection wells [2–5]. Specifically for the following aspects: (1) The production wells with dynamic fractures have a stepwise increase in water content, with liquid increases and oil production rate dropping rapidly. The injection volume and apparent index of the connected injection wells also increase rapidly, but the oil pressure remains basically unchanged; (2) the water injection profile is characterized by a peak shape water intake volume, the API of isotope for water injection profile is larger than 500, the peak value and intensity of the isotope are more than three times of the average value; the water injection index curves often exhibit break points when dynamic fracture occurs and the water intake capacity at the point changes significantly (Fig. 2); (3) the well test analysis shows the characteristics of fracture seepage; time-lapse well indicates that during the water injection process, the fracture half-length is increasing and is more than 200 m. The effective permeability of well test interpretation twice as large as the core permeability; and (4) tracer monitoring has obvious orientation.
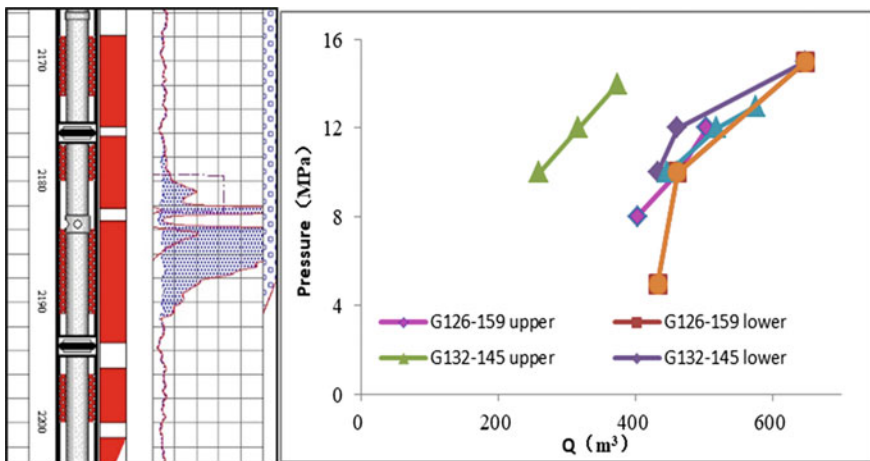

Fig. 2. Injection profile and index curve used to identify dynamic fractures

3.3   Spatial Distribution

In Bai 153 block, there are 43 dynamic fractures identified, and the dynamic fractures are multi-directional, mainly in NE85°, NE105° and NE45°, but with some fractures in other directions.

Vertically, dynamic fractures develop differently in different sand layers. The fractures in Chang 6_3^{12-1} layer are the most developed, with 14 dynamic fractures, followed by Chang 6_3^{11-1} and 6_3^{11-2} layers, and the corresponding number of fractures are eight and six, respectively (Fig. 3). The multi-directional dynamic fractures are

different in lithology section. The dynamic fractures in the direction of NE85° are most developed in calcareous interlayers of the sand debris flow, and some of them are developed in the oil-bearing siltstones, other fractures are multi-directional and generally distributed in the main part of sand debris flow with oil patch.
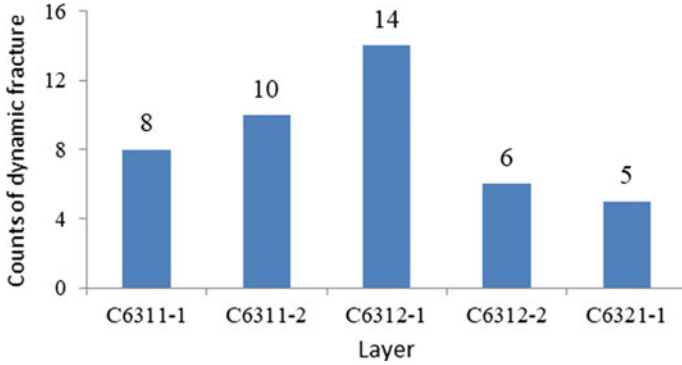

Fig. 3. Distribution of dynamic fractures

In plane, the distribution of dynamic fractures also shows obvious heterogeneity, mostly concentrated in the northern part of the project area, mainly in the direction of NE85° or 105° in northeast, and fractures in NE45° direction in northeast part are rarely developed; the development degree of dynamic fracture is low in south part of B153 block (Fig. 4), and the fractures are only distributed Chang 6_3^{11-1} and Chang 6_3^{11-2}, and the orientation is mostly NE45° and NE150°. The multi-dirsectional dynamic fractures in the non-NE85° direction are mainly developed in the same single sandbody, and the fracture length is not more than one well spacing, about 200 m; the dynamic fractures length in the direction of NE85° is about 900–1000 m, and communicates 2–3 sandy debris flow single sandbodies or turbidity single sandbodies.

3.4　Controlling Factors of Dynamic Fractures Heterogeneity

In the process of water injection in ultra-low permeability reservoirs, the bottom pressure of injection well increases and exceeds the fracture pressure of rocks, dynamic fracture form and continue to extend towards to production wells; besides, the detonation fracturing and compound perforating form fractures of small scale, which are not controlled by the stress. These fractures extend along the direction of the maximum principal stress today to form dynamic cracks [2]. In B153 block, the formation of dynamic fractures is related to the opening of natural fractures. In vertical, the vertical dynamic fracture develops in the layer where natural fractures developed, or the distance from the natural fracture interval to dynamic fracture zone is less than 10 m. In plane, dynamic fractures are mostly located in areas where the natural fracture density is relatively large (Fig. 5). Therefore, the development degree and opening pressure of natural fracture are the main controlling factors affecting the development of dynamic fractures.
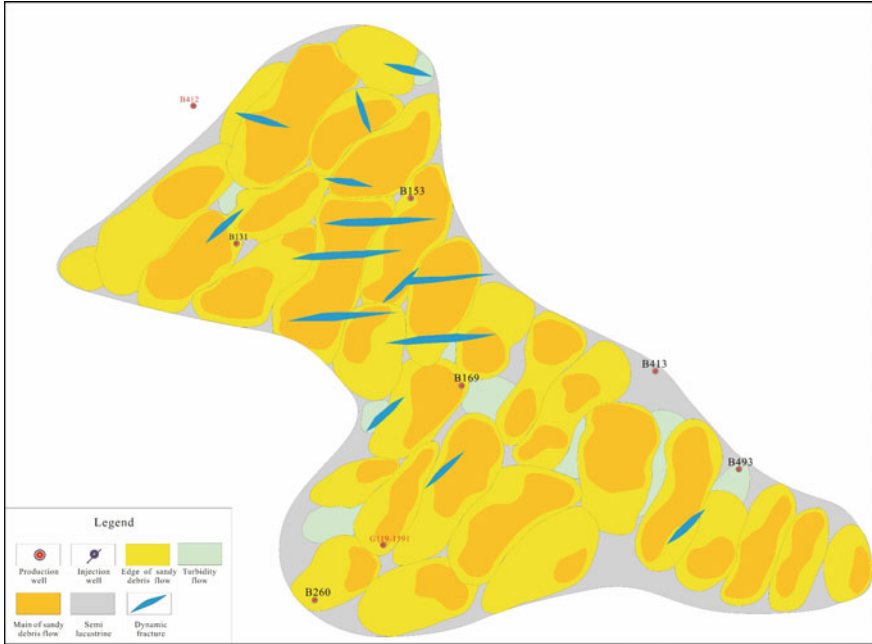
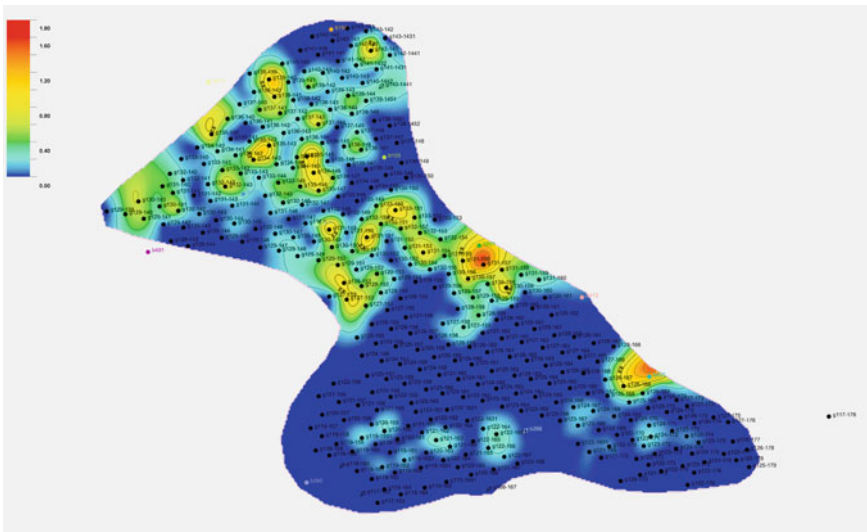**Fig. 4.** Distribution of dynamic fractures in $C6_3^{12-1}$

Fig. 5. Natural fracture density in $C6_3^{12-1}$

Based on core observations and imaging log interpretation results, natural fractures in the B153 block are shear fractures with high angles, small fracture heights and infilling. The dominant fracture orientations are NE-NEE and EW-NWW, followed by NW-NNW. Natural fractures are most developed in calcareous siltstones, followed by siltstones and argillaceous siltstones. They are basically not developed in mudstones. The natural fractures are most developed at the top and bottom of the main part of sandy debris flow body or at the edge part, and the fracture development degree in the turbidity and lacustrine sedimentation is significantly low. Based on the observation of natural fractures in the core, in application of conventional logging curves, natural fractures were identified and predicted by the multi-fractal and neural network quantitative method [6]. The results indicate that natural fractures are mainly distributed in the northern part of the study area and dotted scattered in the south area.

The opening pressure of natural fractures is related to the direction of the natural fracture, the orientation of the maximum principal stress and the angle between these two factors, and the smaller the angle between the fracture strike and the maximum horizontal principal stress, the easier it is to open [7]. Zeng Lianbo (2009) [8] proposed a formula to calculate the pressure required to open natural fractures in different strike orientations, which is applied in Chang 6_3 reservoir in B153 block (Table 1). When calculated, the fracture dip (θ), Poisson's ratio (μ), buried depth, recent minimum ($f_{\sigma3}$) and maximum principal stress ($f_{\sigma1}$), water density ($\rho_W = 1.13$) and rock density($\rho_S = 2.52$) is defined to be a constant, but the angle (β) between fracture trend and recent maximum principal pressure is different.

Table 1. Opening pressure of natural fracture

θ (°)	μ	$f_{\sigma1}$ (MPa/km)	$f_{\sigma3}$ (MPa/km)	β (°)	Open pressure (MPa)
90	0.1989	26	15	5	26.1
90	0.1989	26	15	10	30.6
90	0.1989	26	15	15	34.7
90	0.1989	26	15	20	38.5
90	0.1989	26	15	25	41.9
90	0.1989	26	15	30	45.0

According to the calculation results, natural fractures with angle less than 15° from the direction of the maximum principal stress can be opened to form dynamic cracks. Therefore, natural fractures in the direction of NE75°-85° can be preferentially opened to form dynamic fractures with a bottom pressure of 35 MPa. Afterwards, as the bottom pressure of the injection well increases, dynamic fractures in other directions are opened one after another, forming the current multi-directional dynamic fractures. In addition, it is necessary to further explain that the opening pressure of natural fractures is directly proportional to the depth of burial. With the increase of burial

depth, the pressure required for the opening of natural fractures increases. Therefore, under the precondition that other geological conditions are consistent, and the upper part of Chang 6_3 is more likely to develop dynamic fractures in multiple directions than the lower part.

4 Heterogeneity Characterizations of Matrix Reservoirs

4.1 Reservoir Architecture of Chang 6_3 Thick Sand

Chang6_3 reservoirs of Bai 153 block are mainly deep gravity flow deposits. Based on sedimentary facies research, it is possible to identify sandy debris flow and turbidity sand bodies. Sandy debris flow reservoirs are further divided into the main part of sand debris flow and the edge of sandy debris flow deposition (Fig. 4). The average thickness of Chang 6_3 reservoir is 25.3 m, which is widely distributed within the whole study area. The single sandbody of sandy debris flow and turbidity are vertically overlapped and laterally assembled, and the reservoir complex extends from the northeast to southwest. The barrier lithology is mainly mudstone and argillaceous siltstone; the interlayer lithology is argillaceous siltstone and calcareous siltstone.

Controlled by fluctuation of lake level, the complex sand bodies are spatially superposed and distributed in three ways: isolated, assembled and superposed. At the stage of lake level rising (Chang 6_3^3), the A/S is relatively large, sand debris flow and turbidity sand bodies are isolated from each other, and there is no connectivity between them; after the lake level falling (Chang6_3^2), the A/S decreases, and the spatial superposition pattern is assemble, that is, part of sandy debris flow and turbidity reservoir are pieced together, and the connectivity is weak. As the lake level continues to fall down (Chang 6_3^1), the A/S decreases rapidly and the source supply is abundant enough, the single sand bodies are stacked in multiple stages of sand debris flow, and the turbidity flow is basically not developed. At this time, the space superposition pattern is the main type, and the sand bodies are connected to each other. Different types of spatial distribution of complex sandbodies reflect differences in the connectivity, which provides a geological basis for water injection in spatial.

4.2 Connectivity of Sandbodies

There are three types of vertical communication models of sand bodies, including disconnected, weakly connected and well connected. For disconnected type, the sandy debris flow of different phases or single sandbody of turbidity is separated by a mudstone interlayer and does not communicate with each other; For weak-connected type, single sandbody of sandy debris flow is in direct contact with the turbidity flow, or the contact area of the two-stage sandy debris flow sandbodies is very limited. The connected type refers to the superimposition or lateral overlap of single sand bodies in two stages of sand debris flow. The contact area is large, and the degree of communication between them is high (Fig. 6).
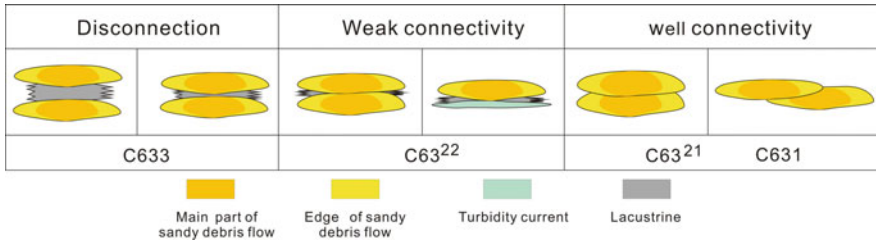
Disconnection	Weak connectivity	well connectivity

C633   C63^{22} C63^{21} C631

Main part of sandy debris flow   Edge of sandy debris flow   Turbidity current   Lacustrine

Fig. 6. Connectivity of single sandbodies in Chang 6_3

4.3 Heterogeneity within a Single Sandbody

The lithology of the main part of sandy debris flow is dominated by grey-brown massive oil trace siltstones, with a homogeneous rhythm or a positive composite rhythm. The average porosity is 10.7%, and the average permeability is 0.2×10^{-3} μm^2. The average permeability ratio is 14.61, and the heterogeneity coefficient of permeability is 2.5. Its heterogeneity is weak. The lithology at the edge of the sandy debris flow is dominated by grey-brown oil trace siltstone, with a positive rhythm. The grain size becomes finer upward, and the mud content increases. The average porosity of that is 9.54%, the average permeability is 0.16×10^{-3} μm^2, the permeability ratio is 24.99 and the coefficient of permeability is 3, its heterogeneity degree is stronger than the main body.

The turbidity current flow deposits mainly develop positive rhythms, and the lithology is greyish brown siltstone or muddy siltstone with argillaceous stripes at the top. The average porosity is 7.79%, the permeability is 0.08×10^{-3} μm^2, the permeability ratio is 29.66, the permeability coefficient is 4.05, and the heterogeneity is stronger than the sandy debris flow.

4.4 Heterogeneity of Interlayers

The interlayers in B153 block mainly include argillaceous and calcareous interlayers. The argillaceous interlayers develop between two stages of single sandbody (Fig. 6), which correspond to the fourth-order interface of reservoir configurations, and divide the sandy debris flow or turbidity current sedimentation of different stages. The average single layer thickness of this type of muddy interlayer is 0.84 m; besides that, it can be observed within single sandbody of the edge of sandy debris flow, with an average single layer thickness of 0.22 m, which is relatively thinner. In plane, the argillaceous interlayer thickness is generally less than 4 m, with a lenticular distribution. It is widely distributed in Chang 6_3^{11-1}, Chang 6_3^{22-1} and Chang 6_3^{22-2}.

On the top of the sandy debris flow sandbody or the bottom of the turbidity current deposits, there can develop 1–2 layers of calcareous interlayers with an average thickness of 0.39 m. The distribution of calcareous interlayers is discontinuous and random and extends in 1–2 well spaces, about 400 metres. In plane, it is scattered distributed, like a patch, and the development degree of calcareous interlayers is relatively low in Chang 6_3^{22-1} and Chang 6_3^{22-2}.

5 Dynamic Fracture-Matrix Comprehensive Heterogeneity and Remaining Oil Model

5.1 Remaining Oil Distribution Control Factors

5.1.1 Permeability Heterogeneity

Due to the variance of permeability in different single sand bodies, in the process of waterflood injection, the injected water penetrates along the high-permeability layer, like the main part of sandy debris flow sandbody, while the low-permeability layer has relatively poor waterflood effect, such as the edge of sandy debris flow and the turbidity sandbody and the remaining oil is retained in there. In plane, the injected water enters the main part of the sandy debris flow with relatively high permeability, and the injection velocity is 24–28 m/d, resulting in water flooding of the wells along the direction of the source, and perpendicular to the source, reservoirs have poor water flood effect and remaining oil was kept in there.

The rhythm of the main part of the sandy debris flow is characterized by uniform rhythm, there is no significant difference in permeability, and with a uniform water injection; the edge of sandy debris flow is positive rhythm, permeability on the top is larger than that of the bottom, so the volume of injected water is bigger than that of the bottom, and the upper reservoir is not fully displaced, remaining oil can be found there (Fig. 7).

5.1.2 Reservoir Configurations

The superposition pattern of single sand bodies has a significant control over the remaining oil distribution.

(1) Spatial superposition pattern

In plane, the single sand bodies of different origin, which deposited at the same time, are overlapped between each other (Fig. 8a, b, and c), and the remaining oil is mainly distributed in the fringe zone where the sand debris flow is converting to the mudstone (Fig. 8c); in vertical, the stacking patterns of different periods of sandy debris flow sandbodies are mainly superposed style, followed by isolated style, the remaining oil may be located on one side of the sandy debris flow single sandbody or fringe zone of both sides (Fig. 8d).

(2) Spatial assembled pattern

In this model, the single sandbody of debris flow and the turbidity are pieced together in plane and in vertical. Due to the difference of permeability between these two bodies, the injection water preferentially runs in sandy debris flow single sandbody. So, the remaining oil is enriched in turbidite sand bodies that are in contact with the sandy debris flow (Fig. 8e, f).

(3) Spatial isolated pattern

Single sandbodies of sandy debris flow or turbidity current are isolated from each other, surrounded by lacustrine mudstone. Under the premise of good well network configuration, each sand debris flow reservoir will be effectively developed with water
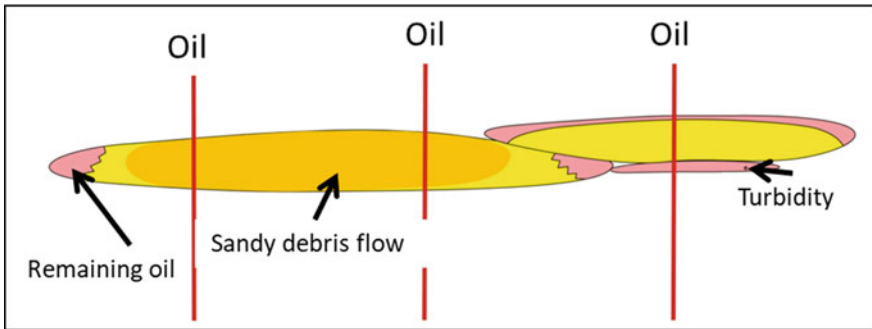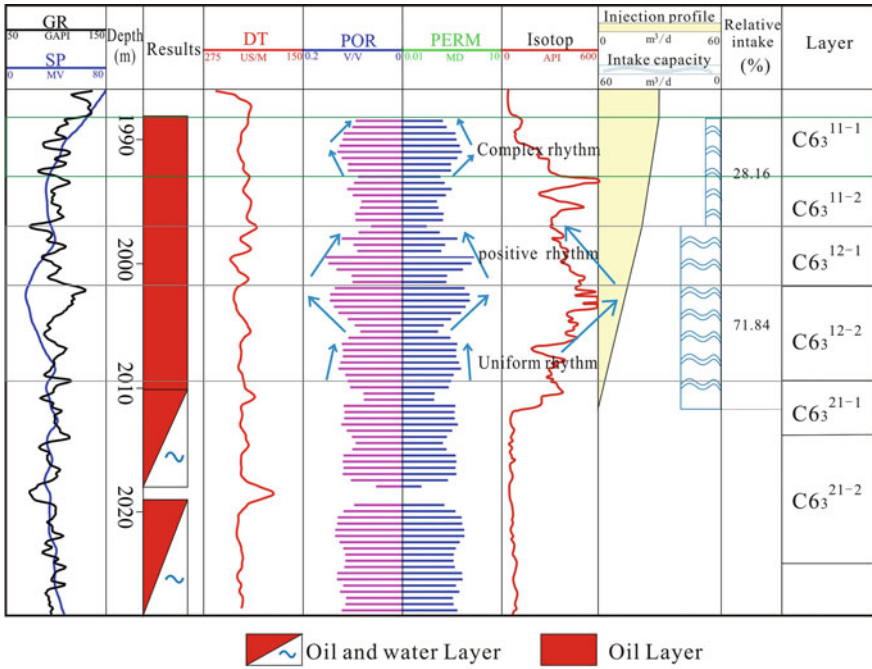
Fig. 7. Effect of the permeability heterogeneity on the remaining oil distribution

injection, and the remaining oil may be enriched in the lateral edge of the sandy debris flow tongue (Fig. 8g); while in the case of an imperfect well pattern, due to the disconnection of sandbodies, the injected well maybe penetrate one single sandbody, but the production well maybe drill another one, so, this will cause the entire hydrocarbon in sandy debris flow reservoir is not exploited.

5.1.3 Interlayers

The argillaceous interlayer in Chang 6_3 reservoir develops at the top or bottom of a single sandbody of sandy debris flow and the calcareous interlayer often develops at the top and bottom of a single sandbody of sandy debris flow. In multilayer water flooding
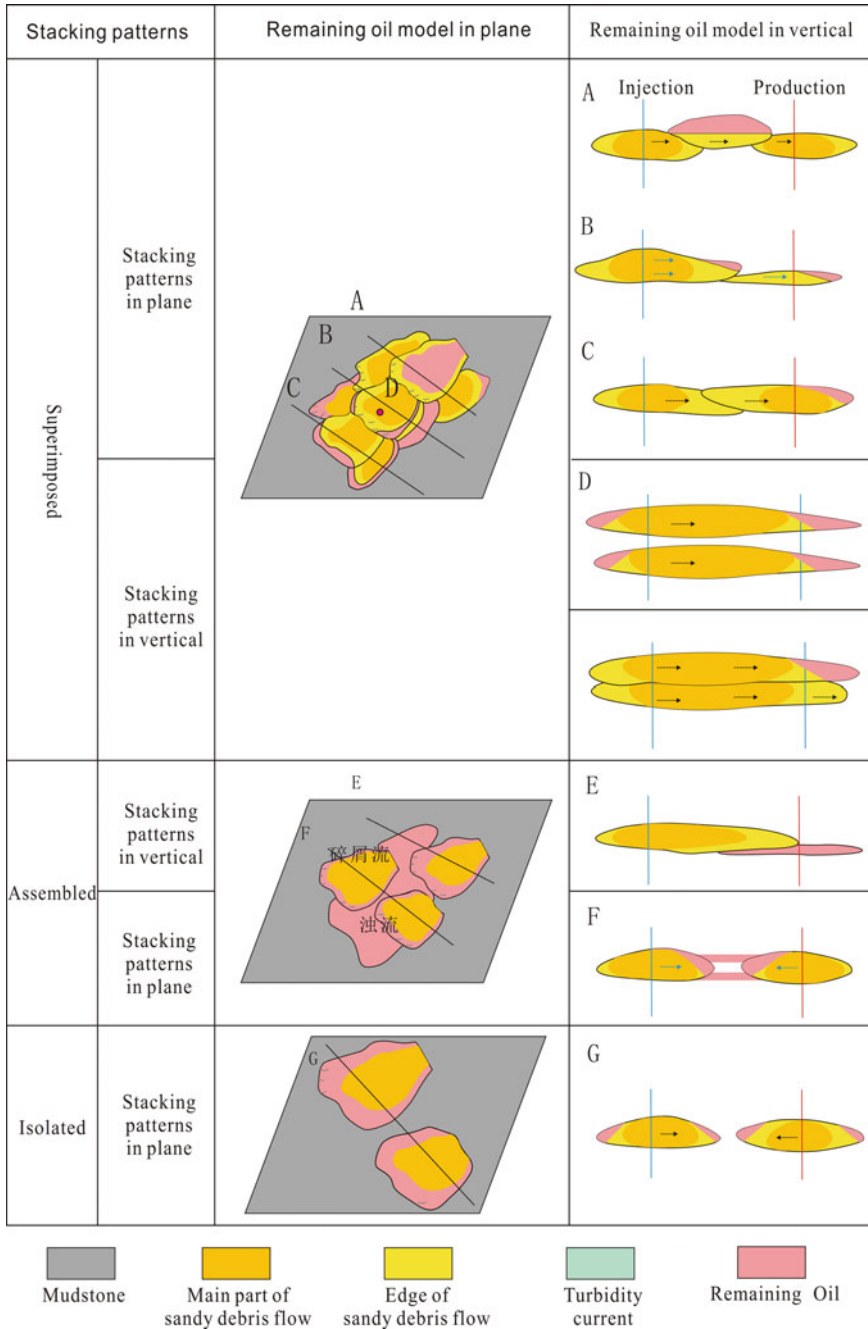
Fig. 8. Effect of the reservoir architectures on the remaining oil distribution

process, if the water injection interval is located in the upper part, and there is a thin layer of calcareous interlayer or argillaceous interlayer between the upper and lower part of single sand bodies, the injection water will be blocked to moving downward. Remaining oil is formed inside the lower part of a single sandbody of sandy debris flow.

5.1.4   Dynamic Fractures

The permeability of dynamic fracture is ten or even times more than that of the matrix reservoir and shows a strong heterogeneity compared with the surrounding matrix reservoir. During the stage of water injection, the injected water runs along the strike direction of the dynamic fracture, forming a linear high-water flooding zone. The matrix reservoir on both sides of the dynamic fracture has poor waterflood efficiency, where the remaining oil is rich (Fig. 9). In the profile, dynamic fractures and matrix permeability differ greatly, and interlayer interference is serious. From the injection profile, it can be seen that the dynamic fracture zones behave as peak shape and with serious water flooding, however, the efficiency of water injection in matrix reservoir is bad. So, the remaining oil stays in the matrix reservoir above and below the dynamic fracture.
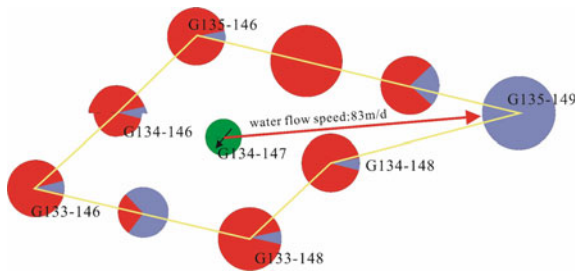

Fig. 9. Effect of the dynamic fracture on the remaining oil distribution

5.2   Combination Model of Dynamic Fracture and Matrix Reservoir and Remaining Oil Distribution

The formation of dynamic fractures is closely related to the opening of natural fractures and is controlled by the scale and development of natural fractures, the current maximum horizontal principal stress, and the injection pressure. The development degree of natural fractures in the area is relevant to reservoir sedimentary facies, lithology and rock brittleness. Therefore, based on the study of the distribution of dynamic fractures, with reservoir performance dynamic analysis, this study discussed the relationship between dynamic fracture positions and natural fractures and matrix reservoir parameters. There are four types of combination of dynamic fractures and matrix reservoirs, with four relevant remaining oil distribution models (Fig. 10).
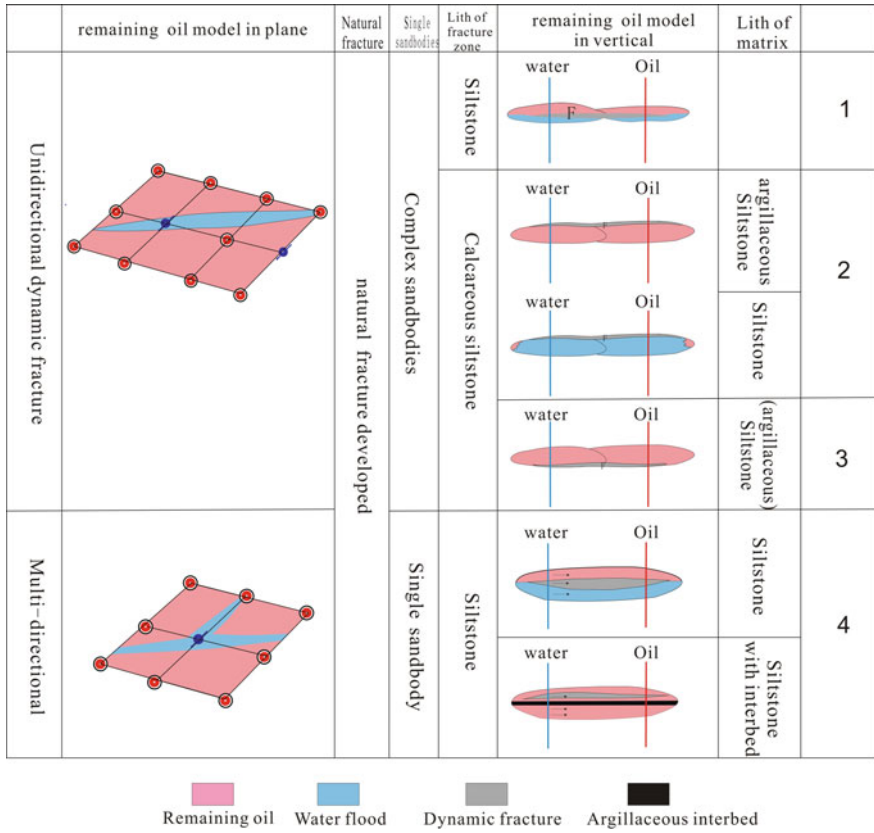
Fig. 10. Comprehensive remaining oil models of dynamic fracture and reservoir matrix heterogeneity

5.2.1 Dynamic Fracture—Natural Fracture (Siltstone)—Siltstone—Composite Sand Bodies Remaining Oil Model

In plane, the extension direction of dynamic fractures is mainly NE85°, and the fracture length is relatively large. Usually, it cuts through 2–3 sandy debris flow sand bodies; in vertical, the dynamic fracture develops in the upper siltstone of the main part of sandy debris flow, and the lithology of the upper and lower matrix reservoirs is a relatively high permeability siltstone (Fig. 11).

In this model, the wells along the strike direction of the dynamic fracture suffer serious water flooding, and the wells perpendicular to the strike direction are not swept or ineffectively swept, resulting in the enrichment of the remaining oil. From water injection profile, the water absorption capacity of the dynamic fracture zone is significantly higher than that of the matrix reservoir, and the interlayer interference phenomenon is serious. Therefore, in vertical, affected by the rapid flooding and gravity effects of dynamic fractures, the reservoir above dynamic fractures is full of remaining oils.
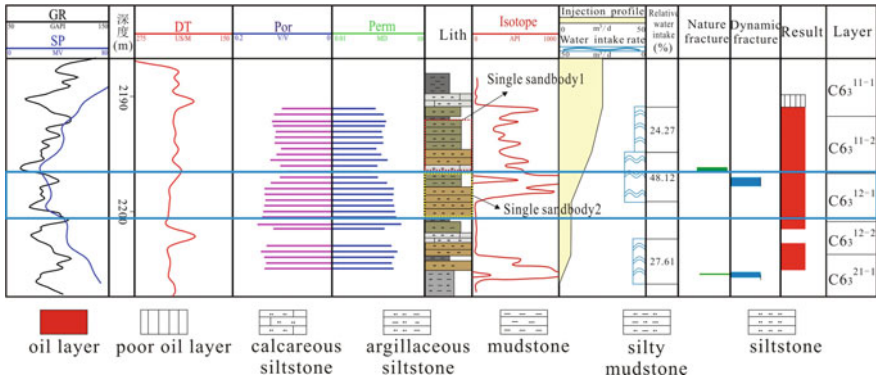
Fig. 11. Remaining oil model integrating dynamic fracture, natural fracture (located in siltstone), siltstone and composite sand bodies, well G132-151

5.2.2 Dynamic Fracture—Natural Fracture (Top Calcareous Siltstone)—(Argillaceous) Siltstone—Composite Sand Bodies Remaining Oil Model

The strike direction of dynamic fractures is NE85°, which intersect 2–3 sandy debris flow single sand bodies; in section profile, natural fractures develop in the dynamic fractures zone, and dynamic fractures are found in calcareous siltstone, at the top or middle part of the sandy debris flow reservoir; the lithology of the matrix reservoir around the dynamic fracture is mainly siltstone or argillaceous siltstone, and its physical properties are relatively good (Fig. 12).
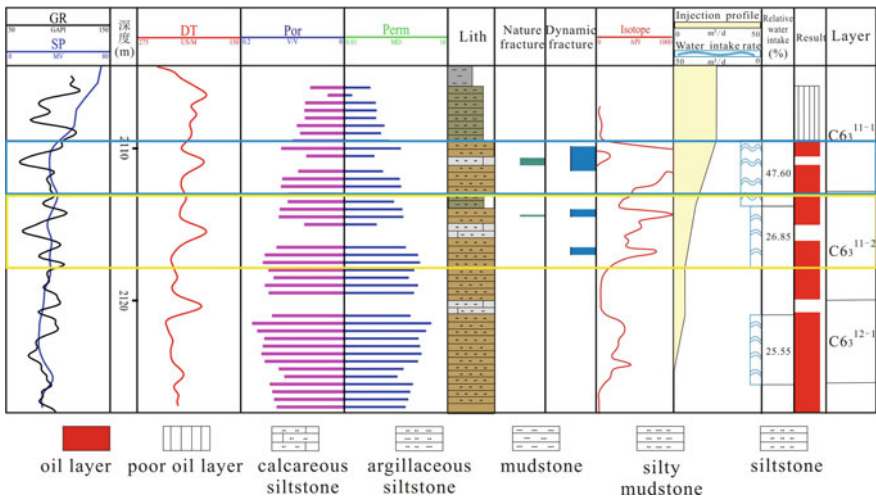

Fig. 12. Remaining oil model integrating dynamic fracture, natural fracture (located in top calcareous siltstone), siltstone and composite sand bodies, well G134-147

In this model, the whole sandy debris flow reservoir may be watered out, and the remaining oil mainly accumulates in both sides of the sandy debris flow reservoir, which is close to the mudstone; however, if the matrix reservoir below dynamic fractures is argillaceous siltstone, with relatively poor physical properties, the injected water is preferentially runs along dynamic fractures, and it is difficult to enter into the lower matrix reservoir. The remaining oil is mainly distributed in argillaceous siltstone where dynamic fractures are not developed. Among them, the plane remaining oil is still distributed in both sides of the fracture.

5.2.3 Dynamic Fracture—Natural Fracture (Bottom Calcareous Siltstone)—(Argillaceous) Siltstone—Composite Sandstones Remaining Oil Model

In plane, the strike direction of the dynamic fracture is still NE85°, which intersects 2–3 sandy debris single sand bodies; in vertical, the dynamic fractures occur in the zone where natural fractures are developed and located in calcareous siltstone at the bottom or the lower part of single sand bodies of sandy debris flow; the lithology of the upper matrix reservoir above dynamic fracture is dominated by argillaceous siltstone, followed by siltstone.

In this model, directional water flooding occurs along the dynamic fractures at the bottom of sandy debris flow, while the sweep efficiency of matrix reservoir above the dynamic fracture is very low, and a large amount of remaining oil is abundant in it. In plane, the remaining oil mainly distributes on both sides of the dynamic fractures.

5.2.4 Dynamic Fracture—Natural Fracture (Siltstone)—Siltstone—Single Sandbody Remaining Oil Model

The dynamic fractures in this model are multi-directional, mainly including NE85° and NE45°, and the latter is dominant. In plane, the dynamic fractures have a short fracture length and generally only develop within a single sandy debris flow reservoir. Dynamic fractures develop in siltstones of the main part of the sandy debris flow, which have relatively good physical properties. The lithology of the matrix reservoir around dynamic fractures is siltstone, and in some wells it is calcareous siltstone (Fig. 13).
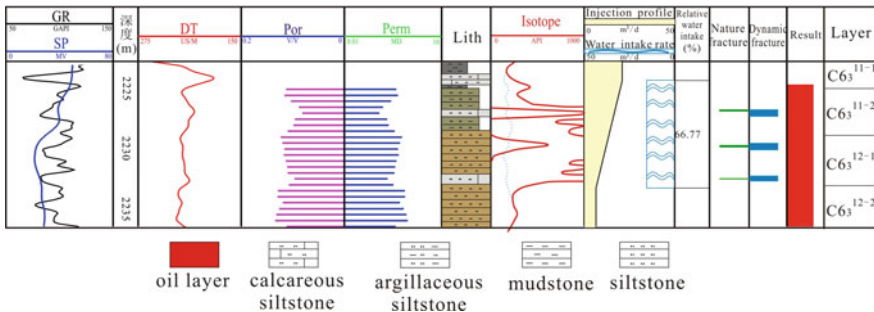

Fig. 13. Remaining oil model integrating dynamic fracture, natural fracture (located in siltstone), siltstone and single sandbody, well G126-155

In this model, the remaining oil is mainly distributed in the sandy debris flow reservoir above the dynamic fracture. In addition, if a thin layer of calcareous or argillaceous interlayer develops within the sandy debris flow, the remaining oil is more likely to develop in the zone close to interbred and the dynamic fractures; in plane, the remaining oil mainly distributed on both sides of the fractures or the cross area of two sets of fractures.

6   Conclusions

(1) The dynamic fractures are developed in north part of project area, with is closely related to the opening of natural fractures. Affected by the dynamic fractures, the injected water runs along the fracture zones, which leads to the low plane sweep efficiency of two sides perpendicular to the fracture, resulting in the accumulation of oil.

(2) Chang 6_3 thick reservoir is composed of complex sandbodies of sandy debris flow and turbidity current, and the permeability variations of different genesis sandbodies and the architecture of the reservoir lead to strong reservoir heterogeneity.

(3) Based on the characteristics and distribution of dynamic fractures and nature fractures, the relationship between the dynamic fracture and the sedimentary facies, single sandbody configurations, and the reservoir heterogeneity parameters is clearly pointed out and establishes four complex remaining oil distribution models of dynamic fractures and matrix heterogeneity.

References

1. Zhang FL. Relation of multicycles to oil and natural gas in the Ordos basin. Petrol Geol Exp. 2004;26(2):138–42.
2. Wang YJ, Song XM, Tian CB, Shi CF, Li JH, Hui G, Hou JF, Gao CN, Wang XJ, Liu P. Dynamic fractures are an emerging new development geological attribute in water-flooding development of ultra-low permeability reservoirs. Petrol Explor Dev. 2015;42 (02):222–8.
3. Gadde PB, Sharma MM. Growing injection well fractures and their impact on waterflood performance. In: SPE annual technical conference and exhibition, 2001.
4. Perkins TK, Gonzalez JA. The effect of thermoelastic stresses on injection well fracturing SPE 11332-PA, 1985.
5. Van den Hoek PJ, Hustedt B, Sobera M. Dynamic induced fractures in waterfloods and EOR, SPE 115204, 2008.
6. Prioul R, Jocker J. Fracture characterization at multiple scales using borehole images, sonic logs, and walk around vertical seismic profile. AAPG Bull. 2009;93(11):1503–16.

7. Zeng LB, Gao CY, Qi JF. The distribution rule and seepage effect of the fractures in the ultra-low permeability sandstone reservoir in east Gansu Province, Ordos Basin. Sci China Ser D Earth Sci. 2008;51:44–52.
8. Zeng LB, Li XY. Fractures in sandstone reservoirs with ultra-low permeability: a case study of the Upper Triassic Yanchang formation in the Ordos Basin, China. AAPG Bull. 2009;93 (4):461–77.